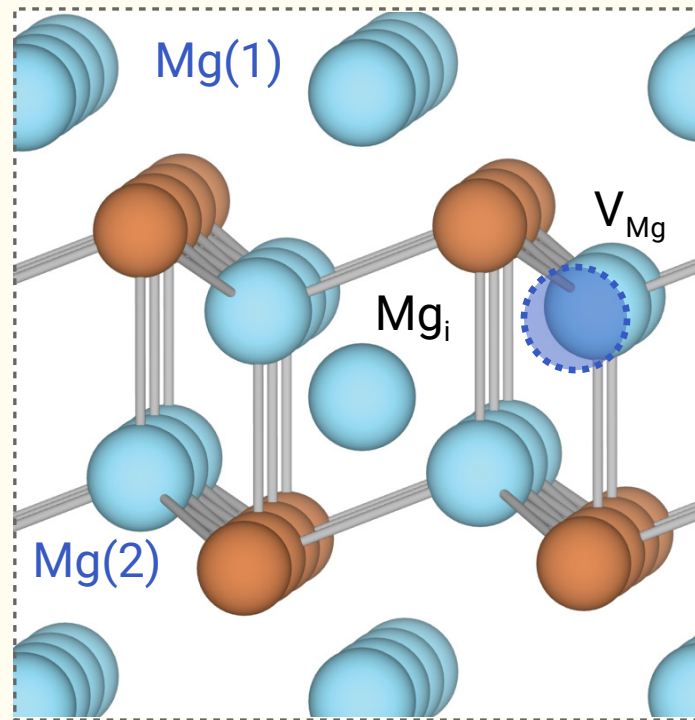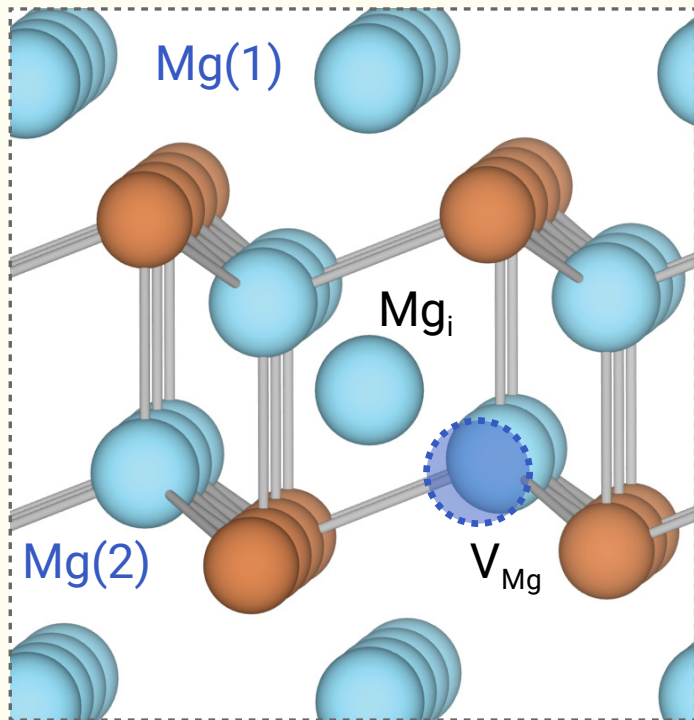# Mg Defect Complexes in Mg$_3$Sb$_2$

Let's Uncomplicate: Mg Complexes in Mg$_3$Sb$_2$

Prashun Gorai[a*] and Vladan Stevanović[a*]

A Comment on "Understanding the Intrinsic p-Type Behavior and Phase Stability of Thermoelectric α-Mg$_3$Sb$_2$" (Chong *et al.*, *ACS Applied Energy Materials* **1**, 6600, 2018).

Mg$_3$Sb$_2$ has risen to prominence as a high-performing thermoelectric material,[1–4] in part due to its successful *n*-type doping under Mg-rich (Mg-excess) growth conditions. It has been theoretically demonstrated that Mg-rich growth conditions suppress the formation of electron-compensating Mg vacancies, which otherwise act as "killer" defects limiting *n*-type doping. In a recent article, Chong *et al.* challenged the role of Mg-rich growth conditions in suppressing Mg vacancy formation.[5] The authors claim that a Mg defect complex $(V_{Mg} + Mg_i)^{1-}$ is the dominant defect under Mg-rich conditions; the excess Mg compensates the defect complexes rather than the Mg vacancies. We regret to inform that there are serious shortcomings in the methodology and results of this paper. Since *n*-type doping is one of the significant issues in the development of Mg$_3$Sb$_2$-based thermoelectric materials, we believe that any contradictions and inaccuracies should be pointed out for clarification. In this comment, we raise four specific concerns regarding the results presented in Ref. [5].

1. Band gap is overestimated: Chong *et al.* used density functional theory (DFT) with hybrid functional (HSE06) to calculate the electronic structure of Mg$_3$Sb$_2$. They report an indirect band gap of 0.82 eV (Figure 2b in Ref. [5]), which is claimed to be in fair agreement with optical transmission measurement of 0.96 eV.[6]

Defect formation energies, and therefore, free carrier concentrations are sensitive to the band gap. Mg$_3$Sb$_2$ is an indirect, small band gap semiconductor.[8–10] In an indirect band gap semiconductor, the optical (vertical) gap is larger relative to the fundamental (transport) band gap. The experimentally determined band gap, estimated from the Goldsmid-Sharp (GS) gaps[11–13] for *p*- and *n*-type Mg$_3$Sb$_2$, is 0.46-0.5 eV[7,14] (Figure 1), which is significantly smaller than the optical band gap of 0.96 eV reported in Ref. [6]. In fact, the fundamental band gap estimated from electronic structure calculations performed with DFT methods employing TB-mbJ functional is $\sim$0.5 eV[8] and with more accurate GW-based methods is $\sim$0.45 eV.[1,15,16] It is somewhat surprising that Chong *et al.* obtained almost 2X larger band gap, compared to experimental measurements and other theoretical calculations.

To verify the band gap overestimation, we calculated the electronic structure of Mg$_3$Sb$_2$ with HSE06 functional with default screened Hartree-Fock exchange mixing of 25%. First, the crystal structure of α-Mg$_3$Sb$_2$ was fully relaxed, followed
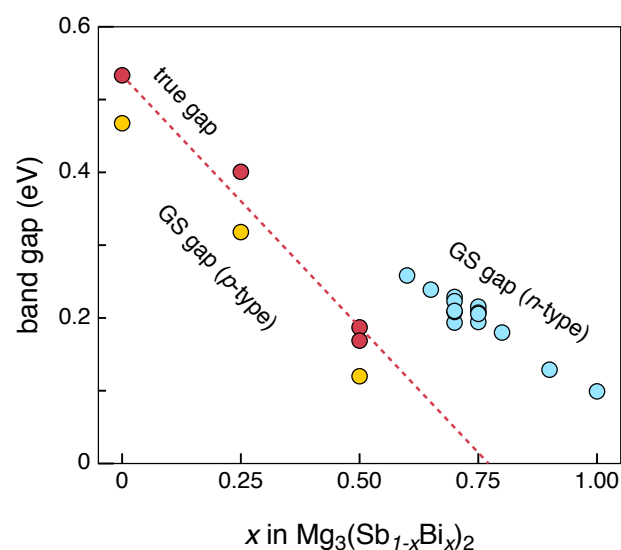

Fig. 1 Experimentally measured band gaps as function of alloy compositions in Mg$_3$(Sb$_{1-x}$Bi$_x$)$_2$. The Goldsmid-Sharp (GS) transport gaps for *n*- and *p*-type are determined from the peak of corresponding Seebeck coefficients with respect to temperature. The estimated true (fundamental) gap is indicated by the dashed line; the true gap of Mg$_3$Sb$_2$ is $\sim$0.5 eV. Data from Ref. [7], reproduced with permission from Royal Soc. Chem.

by calculation of the electronic structure on a dense *k*-point grid (10×10×6). We obtained a fundamental, indirect band gap of 0.53 eV, which is in satisfactory agreement with both experimental measurements as well as calculations based on more accurate GW methods. We are unsure why the band gap (0.82 eV) reported by Chong *et al.* is overestimated by 55% compared to the band gap calculated with the same methodology.

2. Mg complexes are unstable: Chong *et al.* claim that the Mg Frenkel pair complexes $(V_{Mg} + Mg_i)$ are the dominant defects under Mg-rich conditions and that the role of the excess Mg is to compensate the defect complexes.

Due to their complexity, defect complexes are often not considered in first-principles point defect calculations. In some cases, complexes do play a key role in determining the defect properties of materials. For instance, the formation of neutral defect complexes $(2V_{Cu}^{1-} + In_{Cu}^{2+})$ in CuInSe$_2$,[17] a photovoltaic absorber, is believed to give rise to its defect tolerance. *A priori* prediction of likely stable defect complexes is quite challenging. Therefore, we

^{a} *Colorado School of Mines, Golden, CO 80401.* **E-mail: pgorai@mines.edu, vstevano@mines.edu*

(V$_{Mg}$ + Mg$_i$) defect complexes

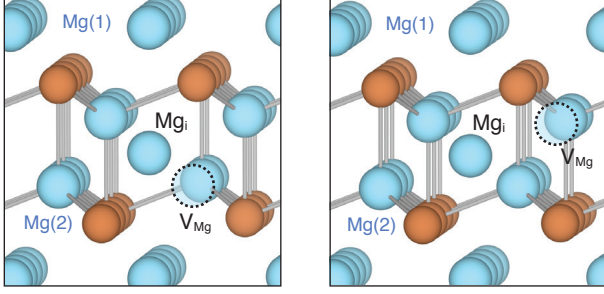**Fig. 2** Two defect complex (V$_{Mg}$ + Mg$_i$) structures showing the stable Mg interstitial in the octahedral site and neighboring Mg(2) vacancies. Mg(1) is the Mg site between the Mg(2)$_2$Sb$_2$ slabs.

Fig. 3 Formation energies ($\Delta H_{D,q}$) of native defects in Mg$_3$Sb$_2$ under Mg-rich growth conditions. Subscripts (1) and (2) denote the unique Wyckoff positions of Mg as shown in Figure 2. The solid vertical line labeled is the conduction band minimum. E_F is the Fermi energy, referenced to the valence band maximum. Figure reproduced from Ref. 15, with permission from Royal Soc. Chem.

appreciate that Chong *et al.* considered a novel defect complex in their defect calculations. In our previously-published defect calculations of Mg$_3$Sb$_2$,[1,15,16] we had not considered defect complexes. We did not suspect the presence of defect complexes since our predictions are in qualitative and quantitative agreement with several independent experimental studies.[1,18–20]

For our own clarification, we investigated the (V$_{Mg}$ + Mg$_i$) complex and attempted to calculate their formation energy. We considered 6 different configurations for the defect complex – the most stable Mg interstitial in the octahedral site and the 6 neighboring Mg sites to create V$_{Mg}$, as shown in Figure 2 for two cases. As a first step, we performed structural relaxations (ionic positions) with density functional theory (DFT) using the GGA-PBE functional,[21] following the methodology previously utilized in Refs. 1,15,16. To our surprise, we found that, upon relaxation, the Mg interstitials spontaneously relax back to the neighboring Mg vacancy site in all 6 cases. consequently, the final relaxed structure is simply pristine Mg$_3$Sb$_2$. Therefore, we find that the defect complex (V$_{Mg}$ + Mg$_i$) is unstable. To further confirm the instability of the complexes, we considered the same defect complex configurations and performed structural relaxations with hybrid DFT functional HSE06 (same methodology as Chong *et al.*[5]); again, we find the defect complexes to be unstable in all 6 cases.

It is not clear how Chong *et al.* obtained the relaxed defect complex structures. We can only speculate that the defect structure is "stuck" in a shallow local minima. Breaking the structural symmetry of the local environment around the Mg interstitial by means of small atomic displacements is likely to "release" the complex structure from the local minima.

3. Charge states of defects are unphysical: Chong *et al.* report defects in multiple charge states (q), including V$_{Mg}$ in q = -3, -4, Mg$_i$ in q = +3, and (V$_{Mg}$ + Mg$_i$) in q = -1.

In standard point defect calculations, it is common to assume a range of charge states for each defect. Depending on the defect type, some of the considered charge states will be inadvertently unphysical. Such unphysical charge states are characterized by charge (electron, hole) filling of the bands (conduction, valence)
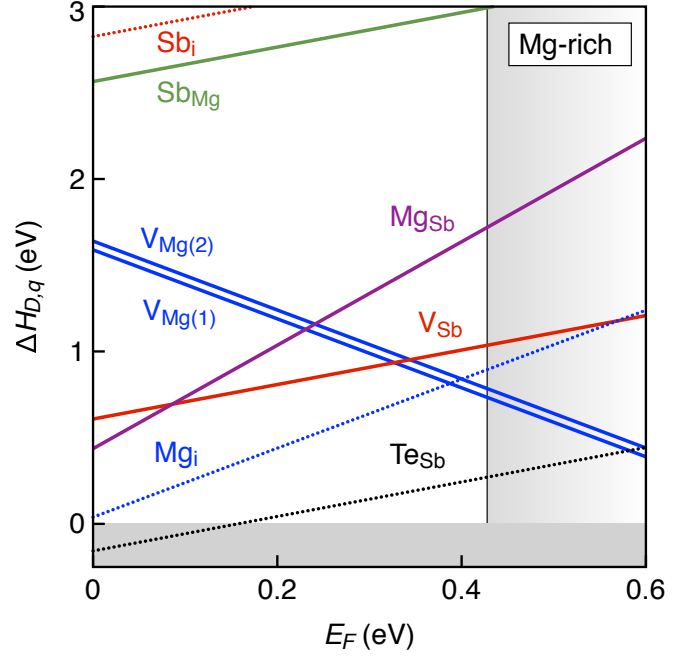
instead of the intended charge localization on the defect site. Inclusion of unphysical charge states in the defect energetics can lead to *qualitatively* inaccurate conclusions. As an example, let us consider Mg$_i$ – when completely ionized, the Mg interstitial can donate up to 2 electrons (3s^2) and convert into a Mg^{2+} ion. However, Mg$_i$ in q = +3 involves formation of Mg^{2+} ions and removal of an electron from the valence band states (alternatively, addition of a hole to the valence band). Therefore, Mg$_i^{3+}$ is an unphysical charge state, and as such, should not be included in the defect energetics. Regarding (V$_{Mg}$ + Mg$_i$), keeping aside the issue of instability of the complex, the -1 charge state of the stoichiometric complex is also unphysical.

4. Doping prediction under Mg-rich conditions is not consistent with experiments: Chong *et al.* predict the native *p*-type self-doping in Mg$_3$Sb$_2$ grown under Mg-poor conditions due to the low formation energy of V$_{Mg}$. Under Mg-rich conditions, V$_{Mg}$ formation energy is relatively higher but still low enough such that the equlibrium Fermi energy is pinned closer to the valence band and Mg$_3$Sb$_2$ is predicted to be doped *p*-type (Figure 4 in Ref. 5)

The defect calculations by Chong *et al.* cannot be reconciled with experimentally observed doping behavior. Previously reported defect calculations of Mg$_3$Sb$_2$ (Figure 3, reproduced from Ref. 15) show that under Mg-rich conditions, V$_{Mg}$ formation energy is high enough to allow extrinsic *n*-type doping with Te and Se, such that the predicted free electron concentrations are

quantitatively consistent with experiments.[1,18] In fact, predictions of effective n-type doping with group-3 elements (Y, La) based on the same defect calculations have been experimentally validated.[18–20] Based on Figure 4 in Ref. 5, Mg_3Sb_2 cannot be doped n-type even under Mg-rich conditions; with extrinsic doping, the equilibrium Fermi energy cannot be pushed beyond 0.4 eV from the valence band maximum (beyond 0.4 eV, V_{Mg} and $V_{Mg}+Mg_i$ formation is exothermic) and as a result, Mg_3Sb_2 cannot be doped n-type, let alone the high free electron concentrations ($>10^{19}$ cm^{-3}) achieved in experiments.

Acknowledgements

References

1 S. Ohno, K. Imasato, S. Anand, H. Tamaki, S. D. Kang, P. Gorai, H. K. Sato, E. S. Toberer, T. Kanno and G. J. Snyder, Phase boundary mapping to obtain n-type Mg_3Sb_2-based thermoelectrics, *Joule*, 2017, **2**, 141.

2 H. Tamaki, H. K. Sato and T. Kanno, Isotropic conduction network and defect chemistry in $Mg_{3+\delta}Sb_2$-based layered Zintl compounds with high thermoelectric performance, *Adv. Mater.*, 2016, **28**, 10182.

3 J. Zhang, L. Song, G. K. H. Madsen, K. F. F. Fischer, W. Zhang, X. Shi and B. B. Iversen, Designing high-performance layered thermoelectric materials through orbital engineering, *Nature Comm.*, 2016, **7**, 1.

4 J. Mao, H. Zhu, Z. Ding, Z. Liu, G. A. Gamage, G. Chen and Z. Ren, High thermoelectric cooling performance of n-type Mg_3Bi_2-based materials, *Science*, 2019, **365**, 495.

5 X. Chong, P.-W. Guan, Y. Wang, S.-L. Shang, J. Paz Soldan Palma, F. Drymiotis, V. A. Ravi, K. E. Star, J.-P. Fleurial and Z.-K. Liu, Understanding the intrinsic p-Type behavior and phase stability of thermoelectric α-Mg_3Sb_2, *ACS Appl. Energy Mater.*, 2018, **1**, 6600.

6 S. H. Kim, C. M. Kim, Y.-K. Hong, K. I. Sim, J. H. Kim, T. Onimaru, T. Takabatake and M.-H. Jung, Thermoelectric properties of $Mg_3Sb_{2-x}Bi_x$ single crystals grown by Bridgman method, *Mater. Res. Express*, 2015, **2**, 055903.

7 K. Imasato, S. D. Kang and G. J. Snyder, Exceptional thermoelectric performance in $Mg_3Sb_{0.6}Bi_{1.4}$ for low-grade waste heat recovery, *Energy Environ. Sci.*, 2019, **12**, 965.

8 J. Zhang and B. B. Iversen, Fermi surface complexity, effective mass, and conduction band alignment in n-type thermoelectric $Mg_3Sb_{2-x}Bi_x$ from first principles calculations, *J. Appl. Phys.*, 2019, **126**, 085104.

9 J. Zhang, L. Song and B. B. Iversen, Insights into the design of thermoelectric Mg_3Sb_2 and its analogs by combining theory and experiment, *Npj Comp. Mater.*, 2019, **5**, 76.

10 D. J. Singh and D. Parker, Electronic and transport properties of Zintl phase $A_eMg_2Pn_2$, Ae=Ca,Sr,Ba, Pn=As,Sb,Bi in relation to Mg_3Sb_2, *J. Appl. Phys.*, 2013, **114**, 143703.

11 H. J. Goldsmid and J. W. Sharp, Estimation of the thermal band gap of a semiconductor from seebeck measurements, *J. Electronic Mater.*, 1999, **28**, 869.

12 Z. M. Gibbs, H.-S. Kim, H. Wang and G. J. Snyder, Band gap estimation from temperature dependent Seebeck measurement - deviations from the $2eS_{max}T_{max}$ relation, *Appl. Phys. Lett.*, 2015, **106**, 022112.

13 J. Schmitt, Z. M. Gibbs, G. J. Snyder and C. Felser, Resolving the true band gap of ZrNiSn half-Heusler thermoelectric materials, *Mater. Horiz.*, 2015, **2**, 68.

14 V. Ponnambalam and D. T. Morelli, On the thermoelectric properties of Zintl compounds $Mg_3Bi_{2-x}Pn_x$ (Pn= P and Sb), *J. Electron. Mat.*, 2013, **42**, 1307.

15 P. Gorai, B. Ortiz, E. S. Toberer and V. Stevanovic, Investigation of n-type Doping Strategies for Mg_3Sb_2, *J. Mater. Chem. A*, 2018, **6**, 13806.

16 P. Gorai, E. S. Toberer and V. Stevanović, Effective n-type doping of Mg_3Sb_2 with group-3 elements, *J. Appl. Phys.*, 2019, **125**, 025105.

17 S. B. Zhang, S.-H. Wei and A. Zunger, Stabilization of ternary compounds via ordered arrays of defect pairs, *Phys. Rev. Lett.*, 1997, **78**, 4059.

18 K. Imasato, M. Wood, J. J. Kuo and G. J. Snyder, Improved stability and high thermoelectric performance through cation site doping in n-type La-doped $Mg_3Sb_{1.5}Bi_{0.5}$, *J. Mater. Chem. A*, 2018, **6**, 19941.

19 S. Song, J. Mao, M. Bordelon, R. He, Y. Wang, J. Shuai, J. Sun, X. Lei, Z. Ren, S. Chen, S. Wilson, K. Nielsch, Q. Zhang and Z. Ren, Joint effect of magnesium and yttrium on enhancing thermoelectric properties of n-type Zintl $Mg_{3+\delta}Y_{0.02}Sb_{1.5}Bi_{0.5}$, *Mater. Today Phys.*, 2019, **8**, 25.

20 X. Shi, T. Zhao, X. Zhang, C. Sun, Z. Chen, S. Lin, W. Li, H. Gu and Y. Pei, Extraordinary n-Type Mg_3SbBi thermoelectrics enabled by yttrium doping, *Adv. Mater.*, 2019, **31**, 1903387.

21 J. P. Perdew, K. Burke and M. Ernzerhof, Generalized gradient approximation made simple, *Phys. Rev. Lett.*, 1996, **77**, 3865.